IJISET - International Journal of Innovative Science, Engineering & Technology, Vol. 7 Issue 6, June 2020
ISSN (Online) 2348 – 7968 | Impact Factor (2020) – 6.72
www.ijiset.com

Effect of Palladium Doping of Photocatalytic activity of Nanostructured CDS

M.J. Pawar *, A.D. Ingale, V.B. Nimbalkar, A.D. Khajone

Laboratory of Materials Synthesis, Department of Chemistry, Smt. Narsamma ACS College, Kiran Nagar, Amravati. M.S. India 444606

Abstract:

The present study exposure undoped CdS and Pd-doped CdS with many concentrations (0-2 Mol%) has been synthesized by hydrothermal method. The resulting samples were characterized by X-ray diffraction, UV-VIS absorption and BET analysis. The results showed absorption spectra of pure and Pd doped CdS nanoparticles recorded within the range 300−700 nm. The position of the absorption spectra is observed to shift toward lower wavelength side in comparison to bulk CdS indicating the blue shift which is a normal trend seen in the nanoscale regime. The photocatalytic activities of samples were evaluated using AB-29 dye as a model organic dye compound under visible irradiation. The results illustrated that the 2% Pd-doped CdS the best photocatalytic activity under visible light irradiation. The results from this work showed that doping with Pd could turn the CdS to become effective photocatalytically active even in visible light. Considering the simplicity in preparation and low cost, this should be an attractive choice to self-cleaning surface.

Keywords: CdS: Pd-doped CdS: Acid Blue 29 Dye: Photocatalytic activity:

1. Introduction

Cadmium sulfide (CdS) has been actively studied for application as a photocatalyst for hydrogen generation from water, as a window layer material for CdS/CdTe solar cells, and for various optoelectronic devices. CdS is one of the most studied materials because it has a well-established relationship between the optical absorption and the size of the particle; the first investigations in this area were focused in the improvement of the synthesis method [1-3]. There are numerous reports on the synthesis of CdS nanoparticles, such as sol-gel [4], chemical vapour deposition [5,6], solvothermal [7,8], spray pyrolysis [9, 10] and microwave (MW) assisted synthesis [11-13]. However, suspension colloidal synthesis routes offer the advantage such as short time reaction and industrial scalable.

The wide band gap limits the use of sunlight as excitation energy and the high rate of recombination of photo-generated electron-hole pairs in CdS results in low photocatalytic efficiency. To overcome these two difficulties, many efforts have been made to modify CdS nanoparticles. One of the promising approaches is based on the metal loading. Various metals, such as Pt, Au, Pd, Rh and Ag, have been used as electron acceptors to separate the photo-induced hole/electron pair and promote interfacial charge-transfer processes. Therefore, the aim of the present work is to study the effect of palladium on the properties and activity of the CdS photocatalyst prepared by the modified hydrothermal method. To investigate the photocatalytic efficiency of the pure and Pd-doped CdS, acid blue dye (AB-29) was used as a model pollutant.

2. Experimental

2.1 Materials

$Cd(NO_3)_2.4H_2O$ was used as the cadmium precursor 1-thioglycerol, Palladium (II) nitrate dehydrate, $(NH_4)_2S$ and NaOH all from Sigma Aldrich were used as obtained for the synthesis of pure and Pd doped CdS nanomaterials.

2.2 Method of synthesis

Pure and Pd-doped CdS (Pd content 0-2% mole fraction) were synthesized by modified hydrothermal method to the process we have adopted for the synthesis of Ag doped CdS samples [14]. Palladium (II) nitrate dehydrate was used as the source of palladium. All the solutions were prepared in deionized water. 100 mL of 0.2 M 1-thioglycerol, 0.1 M $(NH_4)_2S$ solution and 50 mL of 0.1 M NaOH was added slowly to 150 mL of 0.09 M ($Cd(NO_3)_2$) solution and vigorous stirring was continued for 1 hour. To this solution, calculated amount of palladium nitrate was added and the mixture was further stirred for 2 hours. Then the mixture was kept in furnace at 180ºC for 10 hours and then allowed to cool at room temperature. The light yellow precipitates were centrifuged and washed several times using water and ethanol. The final products were dried at room temperature for 4 hours.

2.3 Characterization

The X-ray diffraction (XRD) patterns of prepared films were collected using X-ray diffractometer equipped with Cu $K\alpha$ as a radiation source (λ = 0.154 nm) in the 2θ range (20º - 80º) at a scanning rate of 2° min^{-1}.Optical absorption measurements were

performed using a spectrophotometer in the range from 400 to 700 nm. The photocatalytic experiments were conducted under ambient atmospheric conditions in a reactor using visible light (>360 nm) in dark. In order to ensure adsorption equilibrium, the solution was stirred for about 45 min in dark, prior to irradiation. The apparent kinetics of dye degradation was determined by monitoring the concentration of the substrate using spectrophotometer. The photo degradation efficiency of the CdS samples forAB-29 dye by was calculated using the Equation 1.1.

$$\textbf{\% Degradation} = \frac{C-C_0}{C_0} \qquad \textbf{(1.1)}$$

where, C_o and C are the concentration of the dye before and after exposure to the UV irradiation, respectively.

3. Results and Discussion

3.1 X-ray Diffraction Studies

The X−ray diffraction patterns are shown in Figure 1.1 and were analyzed by powder X-software for pure and Pd doped CdS samples. They all matched with the cubic structure without any impurity phase indicating high purity of the products. The diffraction peaks along with their relative intensities were found to be in good agreement with those reported in JCPDS card no. 10−0454. Three diffraction peaks appearing for all the samples at 2θ values of about 26.67, 43.73 and 51.95 correspond to the (111), (220) and (311) planes of cubic phase of CdS. The peaks (111), (220), (311) observed at Bragg's angle for undoped and Pd doped CdS samples are shown in Table 1.1.

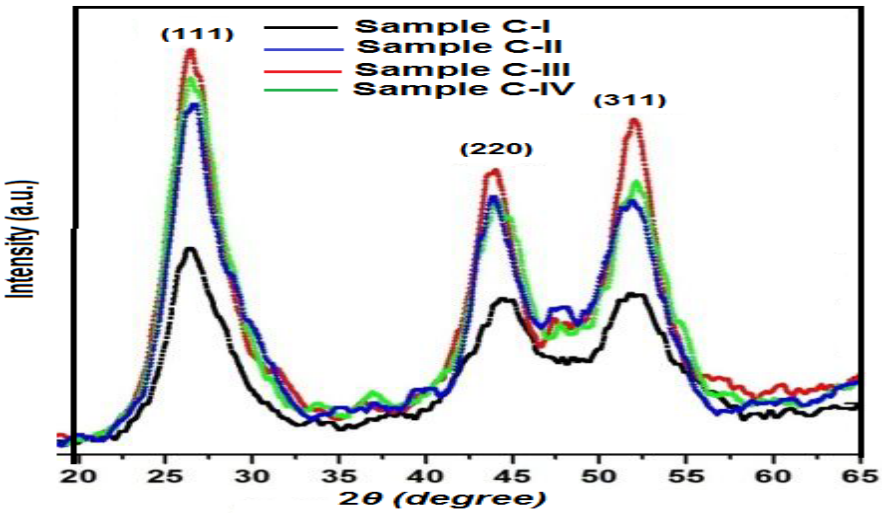

Figure 6.1 XRD spectra of pure and Pd doped CdS samples.

The small shift in the peak position attributed to the local vacancies in the crystal structure [15]. According to Vegard's law, the dopant alone cannot generate an

individual peak by the side of host peak, but it can produce adequate shift in the position of host peak. It was understood that the host has accommodated Pd^{2+} ions into its lattice, since Pd^{2+} possesses smaller ionic radii (86 pm) than Cd ion (97 pm). The further small shifts in the peaks position in Pd doped CdS samples ascertain to the incorporation of Pd^{2+} into the CdS lattice and also exhibits zero alteration in the phase property of CdS. Further the electro negativities of both cations differ with sulphur, (Pauling electronegativity for Pd and Cd are 2.2 and 1.69 respectively) there by suggesting that Pd may get incorporated into the CdS lattice at vacancy sites most probably.

The average crystallite size (D) of the sample is determined to be ~ 5 to 15 nm from the full width at half maximum (FWHM) of the most intense peak making use of the Scherrer equation.

$$\boldsymbol{D = \frac{0.9\lambda}{\beta Cos\theta}} \qquad \textbf{(1.2)}$$

Where, λ is the wavelength of the X-ray radiation, β is the FWHM in radians of the XRD peak and $\theta$is the angle of diffraction. Average crystallite size calculated from XRD has been shown in Table 1.2.

Table 1.1 Structural parameters of undoped and Pd doped CdS samples.

Sample	2θ (degree)			a(Å)	Crystallite size	
	(111)	(220)	(311)		Debye Scherrer's equation	HW plot
C-I	26.42	43.62	51.10	5.86	4.51	5.73
C-II	26.52	43.77	52.13	5.82	6.05	5.30
C-III	26.70	43.61	52.48	5.81	4.91	4.87
C-IV	27.06	44.55	51.90	5.80	3.33	2.99

The calculated lattice parameter value for undoped CdS comes out to be 5.87Å whereas for Pd doped CdS shows slight decrease in lattice parameter with increase of Pd concentration. The average crystallite size determined using full width at half maximum (FWHM) of the diffraction peaks using *Debye Scherrer's* equation 6.3 [14].

3.2 UV−Vis−NIR Spectroscopy

Figure 1.2 shows the absorption spectra of pure and Pd doped CdS nanoparticles recorded within the range 300−700 nm. The position of the absorption spectra is observed to shift toward lower wavelength side in comparison to bulk CdS indicating the blue shift which is a normal trend seen in the nanoscale regime. The optical band gap was calculated using the well-known Tauc relation [16].

$$\alpha h\nu = A(h\nu - Eg)^n \quad (6.3)$$

where, E_g is the band gap corresponding to a particular transition occurring in the material and n characterizes the nature of transition. The value of *n* may be 1/2, 2, 3/2 and 3 corresponding to allowed direct, allowed indirect, forbidden direct and forbidden indirect transitions respectively.

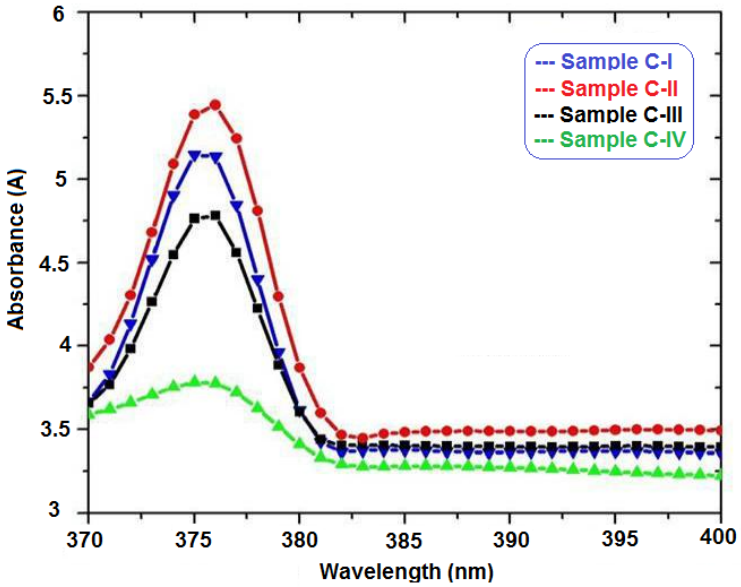

Figure 1.2 UV−Vis−NIR spectra of pure and Pd doped CdS nanoparticles.

Table 1.2 Band gap and particle size of pure and Pd doped CdS nanoparticles.

Samples	Particle size (nm)	Band Gap (eV)
C-I	3.42	3.23
C-II	3.43	3.23
C-III	3.49	3.22
C-IV	3.77	3.13

3.3 BET Surface

The surface areas of the as-synthesized pure and Pd doped CdS samples are characterized by nitrogen adsorption-desorption Brunauer–Emmett–Teller (BET) analysis, as shown in Table 1.3. From the results of BET analysis, the specific surface areas of the samples; C-I, C-II, C-III and C-IV are calculated to be 39.41, 40.36, 41.93 and 42.63 m^2/g respectively. From the above results, it can be seen that the surface area of sample C-IV is slightly higher among all the specimens. This implies that the enhancement of the adsorption capacity occurred in sample C-IV, compared to that of the other samples.

Table 1.3 Brunauer–Emmett–Teller (BET) surface areas of pure and Pd doped CdS nanoparticles

Sample	BET Surface Area (m^2/g)
C-I	39.41
C-II	40.36
C-III	41.93
C-IV	42.63

3.4 Photocatalytic Property

The photocatalytic activity of the synthesized CdS nanoparticles (samples C-I, C-II, C-III and C-IV) was studied by photo-degradation experiment of AB-29 dye in presence of visible light. The blank experiments were also separately carried out by irradiating the aqueous solution of the dye derivative in absence of the photocatalyst and in presence of the photocatalyst under dark condition. Analysis of the samples in both cases did not show any appreciable loss of the dye (Figure 1.4). In order to attain the superior photocatalytic activities of CdS nanoparticles, the activity of all the four samples were compared. The effect of Pd doping in CdS catalyst on the removal of dye was studied and the results are presented in Figure 1.4.

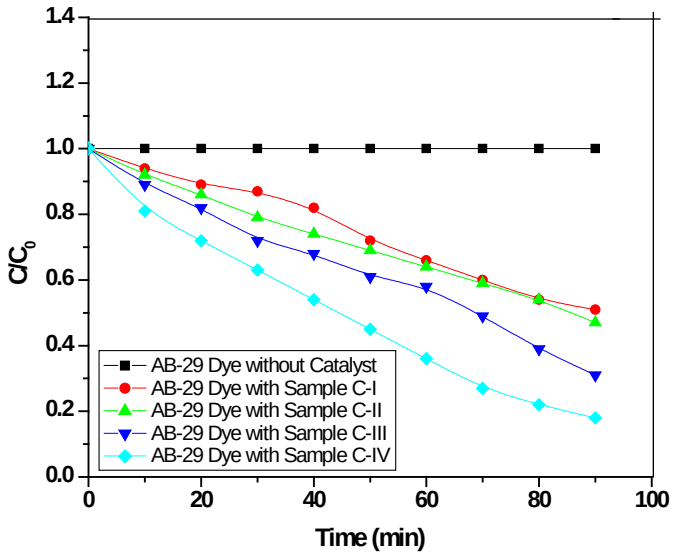

Figure 1.4 Change in concentration of AB-29 dye in absence and presence of CdS samples.

3.4.1 Effect of catalyst dose

The photocatalytic degradation of the AB-29 dye (40 mg/L) with different as synthesized sample C-IV amounts was studied and the obtained results are shown in Figure 1.5.The efficiency of photocatalytic degradation of the dye clearly increased with the increase of the amount of photocatalyst. The concentration of 1.0 g/L of the sample C-IV degraded around 97% of the dye in about 90 min. However, the concentration of0.1 g/L of the sample C-IV in the end of 90 min of irradiation yielded only 22% degradation to that of the highest concentration of the sample used. This can be rationalized in terms of availability of active sites on the Pd doped CdS surface and of the light penetration of photoactivating light into the dye-Pd/CdS suspension; in fact in the dye solution, containing 1.0g/L of Pd/CdS in suspension the light penetration depth is considerably smaller than in those containing only 0.1 g/L of Pd/CdS and so the effect of the increase on the amount of photocatalyst becomes reduced. For the dye studied in this work the treatment with as synthesized CdS samples under artificial irradiation of a visible light was an extremely efficient photodegradation method, since after 90 minAB-29 dye showed substantial degradation.

The photodegradation is mostly promoted by the Pd/CdS catalyst since we observed that direct photolysis, in the 90 min irradiation period, is only responsible for the degradation of the dye. Therefore, under irradiation, only the molecules adsorbed on

the surface of catalyst can be degraded. When the amount of catalyst used on the photocatalytic degradation is very high the turbidity of the suspension strongly inhibits further light penetration in the photoreactor [25, 26].This limit on catalyst amount to be used depends on the geometry and working conditions of the photoreactor which should enable that all the photocatalyst particles present on the entire exposed surface are fully illuminated. In this way, for each system to be remediated thought this method the optimum amount of the catalyst has to be determined in order to avoid the use of unnecessary catalyst in excess and also to ensure the total absorption of the irradiating photons in order to achieve an efficient photodegradation of organic pollutants.

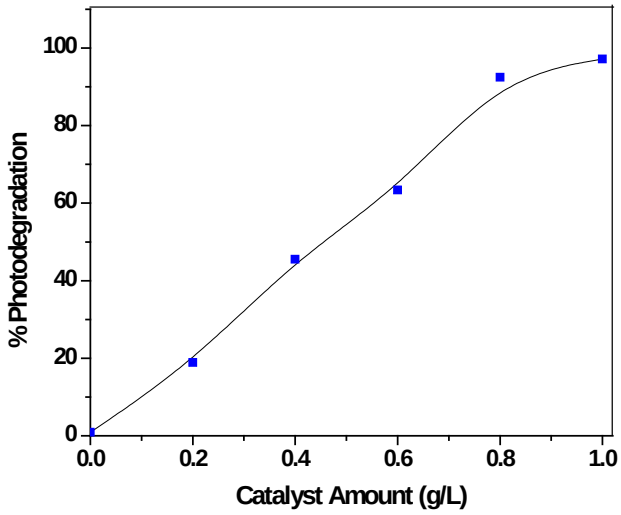

Figure 1.5 Effect of the catalyst (sample C-IV) amount on the complete degradation of 40 mg/L AB-29 dye.

3.4.2 Effect of Dye Concentration

The effect of the initial concentration of AB-29 dye under the reactor was determined. The obtained results are presented in Figure 1.6. The results indicate that the decomposition rate of dye strongly depends on the initial dye concentration. The efficiency of photodegradation of the dye decreased with increase of the initial dye concentration.

On increasing the concentration of the dye until 150 $mg \cdot L^{-1}$the photodegradation became very slow. As the initial concentration of the dye increased, more dye molecules were adsorbed on the surface on the catalyst, consequently the generation of hydroxyl radicals was reduced since the active sites were occupied by dye molecules [18-20]. An increase of the initial dye concentration results in an increase of the amount of dye

adsorbed on the catalyst surface, affecting the catalytic activity of the photocatalyst [21, 22]. Moreover the reduction of the light path length as the concentration and deepness of the colour of the solution rises also cannot be neglected.

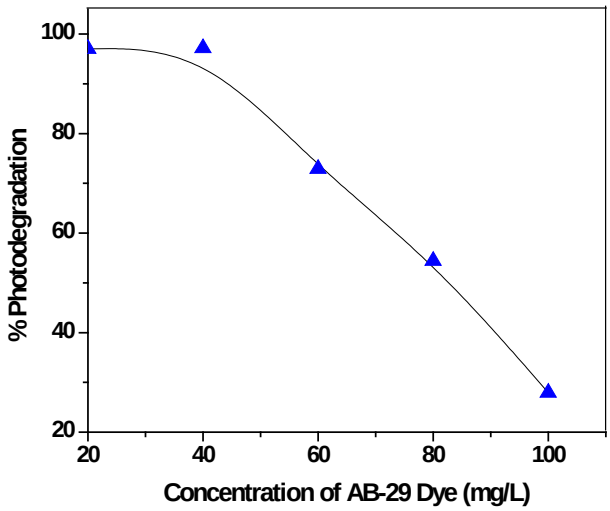

Figure 1.6 Effect of the initial concentration of AB-29 dye on the efficiency attained after 90 min of irradiation with sample C-IV.

3.4.3 Effect of pH

It is well known that the pH of the solution is one of the most important parameters in the photocatalytic degradation of organic compounds. This is attributed to that the pH does not only determine chemical properties of the photocatalyst but also influences adsorption behaviour of the pollutants [23]. Thus the solution pH may be an important operating parameter that might affect the removal efficiency of AB-29 and hence must be fixed.

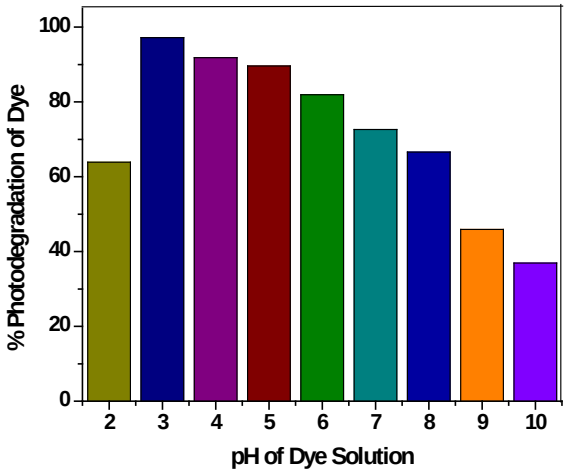

Figure 1.7 Effect of pH of dye solution of photodegradation of Pd doped CdS sample.

The effect of solution pH was studied in the range of 2 to 10 for the optimized catalyst amounts (*i.e.*, 1 g/L) for AB-29 dye under visible light for 90 min while all other parameters remained constant. The pH of the solution is adjusted by addition of 0.01 M HNO_3 and 0.01 M NaOH solutions. *Konstantinou et.al*, has reported that the degradation rate of azo dyes increases with decrease in pH [24]. Figure 1.7depicts the variation of the amount of AB-29 dye adsorbed on the photocatalyst as function of pH at 25˚C. The figure indicates that the amount of dye adsorbed is higher in acidic medium and decrease with increasing initial pH. This result may be due to the influence of the solution pH on both the surface state of Pd doped CdS (sample C-IV) and the ionization state of ionisable organic molecule of the day. It is observed that pH of the medium has remarkable effect on the degradation of dye. Highest degradation was observed at pH 3 followed by pH 5 (97.20 and 89.6%, respectively, in 90 min) and lowest in neutral and basic media. A significantly high electrostatic attraction between the positively charged catalyst surface and anionic dye molecules may favour the adsorption of dye at lower pH. However, at higher pH, highly mobile OH^- ions will be preferred for adsorption on the catalyst surface rather than the bulky dye anions [25].

3.4.4 Effect of Reaction Temperature

As like an initial dye concentration and light intensity possess optimal conditions, an optimal temperature range also exists for photodegradation. Low temperature favors the adsorption of the reactant on the catalyst surface, which is a spontaneous exothermic process, whereas the apparent activation energy increases as the temperature decreases close to 0˚C. Low temperature also favors the adsorption of the final product, albeit while decreasing the number of active sites. Therefore, compared to photodegradation and the adsorption of reactants, the slower desorption of product inhibits the reaction and serves as the rate-limiting step under low reaction temperatures. In contrast, when the temperature increases up to the boiling point of the solvent (water for most of the cases), the exothermic adsorption of reactants becomes disfavored, thus limiting the photodegradation reaction [26]. Charge-carrier recombination is also substantially promoted [27] as the reaction temperature exceeds 80˚C. At higher temperatures, the enhanced kinetic energy of dye molecules might allow them escape from the photocatalyst surface [28], leading to decreased photodegradation efficiency. Thus, the adsorption of dye molecules becomes the limiting step at high temperatures. As a result,

reaction temperatures between 20 and 80˚C [29] are considered as the desired temperature for the effective photodegradation of dye molecules.

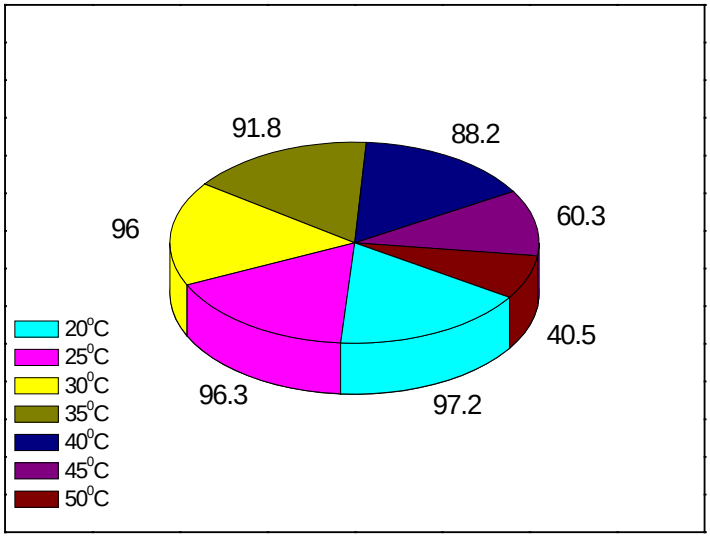

Figure 1.8 Effect of reaction temperature on photodegradation of AB-29 dye over Pd doped CdS sample. (pH of solution 3, catalyst 1 g/L).

In this work, we have tested the effect of reaction temperature on the photodegradation efficiency of sample C-IV keeping all the conditions constant. The results are depicted in Figure 1.8. Figure shows that the highest photodegradation of AB-29 dye is highest at the low temperature 20˚C and lowest at 50˚C. This because, at low temperature rate of adsorption of dye molecules over the catalyst surface is high hence the photodegradation is maximum. Moreover, at high temperature, the rate of adsorption is minimum that results in minimum degradation efficiency of the catalyst. The results are in good agreement with the previous studies.

3.4.5 Effect of Oxidising Agent

Reports show that oxidizing agents have a great deal of influence on the photocatalytic degradation of dyes. The addition of peroxide increases the rate of photodegradation reaction with adequate oxygen supply, because the solution phase may at times be oxygen starved as a result of either oxygen consumption or slow oxygen mass transfer. Other researchers had pointed out as part of their findings that one practical problem in using metal oxides and metal sulfides as photocatalysts is the undesired electron–hole recombination, which in the absence of proper electron acceptor or donor, is extremely efficient and thus represents the major energy-wasting step, thereby limiting the achievable quantum yield. Therefore to inhibit electron–hole recombination,

irreversible electron acceptors are needed by the reaction system. To solve this problem, of $H_2O_2$was found to be beneficial for the photoxidation of the dyes of different chemical groups including azo dyes.

Hydroxide radicals (•OH) formed from $H_2O_2$by reactions with the photogenerated electrons can exert a dual function: as strong oxidant themselves and as electron scavengers, thus inhibiting the electron–hole recombination at the semiconductor surface [30] according to the following equations:

$$H_2O_2 + h\nu \rightarrow 2\bullet OH \quad (1)$$

$$H_2O_2 + e_{CB}^- \rightarrow \bullet OH + OH^- \quad (2)$$

It must be noted that the addition of peroxide increases the rate towards real reaction with adequate oxygen supply, because the solution phase may at times be oxygen starved as a result of either oxygen consumption or slow oxygen mass transfer.

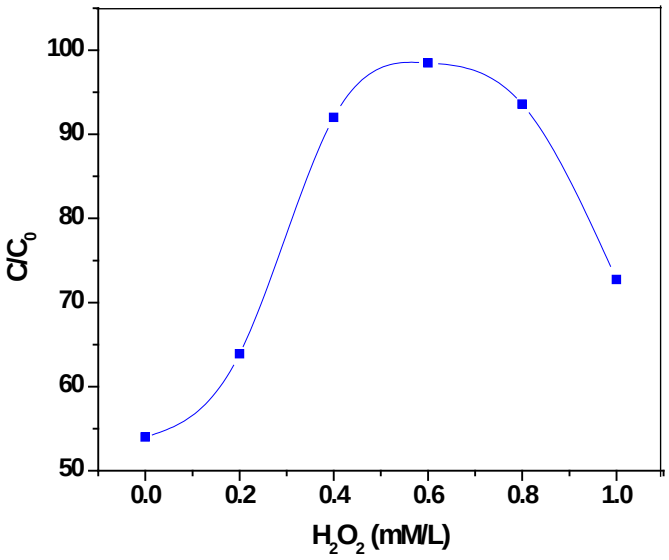

Figure 1.9 Effect of H_2O_2 concentrations (mM/L) on photodegradation of AB-29 dye over sample C-IV under visible light exposed for 40 min.

The experiment was conducted at the concentration range of 0.2–1 mM/L H_2O_2.and the results are presented in Figure 1.9. The % photodegradation of AB-29 dye was found to increase with increase in H_2O_2 concentration. Figure 1.8 depicts that, an optimum addition of 0.6mM/L H_2O_2 for the complete photodegradation of AB-29 dye solution by Pd doped CdS (sample C-IV) in 40 minutes.

At higher dosage of H_2O_2 beyond the optimum, the degradation efficiency of AB-29 dye decreased. This was because the very reactive •OH radicals and valence band

holes (h_{VB}^{+}) could be consumed by H_2O_2 itself as given in the following equations [31, 32]:

$$H_2O_2 + \bullet OH \rightarrow H_2O + HO_2\bullet \quad (3)$$

$$\bullet OH + HO_2\bullet \rightarrow O_2 + H_2O \quad (4)$$

$$H_2O_2 + h_{VB}^{+} \rightarrow 2H^{+} + O_2 \quad (5)$$

$$\bullet OH + \bullet OH \rightarrow H_2O_2 \quad (6)$$

As both •OH and h_{VB}^{+} are strong oxidants for organic pollutants, the photocatalytic degradation of AB-29 dye will be inhibited in the condition of excess of H_2O_2. Furthermore, H_2O_2 can be adsorbed onto Pd doped CdS particles to modify their surfaces and subsequently decrease its catalytic activity [33].

4. Conclusion

In summary, the Pd/CdS nanoparticles were successfully synthesized, and the catalytic activity of Pd/CdS samples was studied. These Pd/CdS metal semiconductors absorb significantly larger amount of visible photons as compared to CdS. Various operational parameters affect the effectiveness or activities of CdS based photocatalysts. It is therefore necessary to study the nature of the sample to be degraded, as this will provide a clue on the type of photocatalyst to be used in its degradation.

5. References

[1] C.B. Murray, D. J. Norris, M. G. Bawendi. J. Am. Chem. Soc. 115, 8706 (1993).

[2] T. Vossmeyer, L. Katsikas, M. Giersig, I. Popovik, K. Diesner, A. Chemseddine, A. Eychmüller, H. Weller. J. Phys. Chem. 98, 7665 (1994).

[3] J. R. Lakowicz, I. Gryczynski, Z. Gryczynski, C. J. Murph. J. Phys. Chem. B. 103, 7613 (1999).

[4] N.V. Hullavarad, and S.S. Hullavarad. Photonics and Nanostructures.15, 156 (2007).

[5] T. Zhai, Z. Gu, H. Zhong, Y. Dong, Y. Ma, H. Fu, Y. Li, J. Yao. Cryst.Growth Des.7(3), 488 (2007).

[6] B J.K. Dongre, V. Nogriya, and M. Ramrakhiani. Appl. Surf. Sci. 255(12), 6115 (2009).

[7] A. Phuruangrat, T. Thongtem, and S. Thongtem.Mater.Lett.63(17), 1562 (2009).

[8] A. Tang, F. Teng, Y. Hou, Y. Wang, F. Tan, S. Qu, and Z. Wang. Appl. Phys. Lett. 96, 163112 (2010).

[9] S.J. Ikhmayies and R.N. Ahmad-Bitar. Appl. Surf. Sci. 255(20), 8470 (2009).

[10] N. Badera, B. Godbole, S.B. Srivastava, P.N. Vishwakarma, L.S. Chandra, D. Jain, M. Gangrade, T. Shripathi, V.G. Sathe,and V. Ganesan. Appl. Surf. Sci. 254, 7042 (2008).

[11] E. Caponetti, D.C. Martino, M. Leone, L. Pedone, M.L. Saladino, and V. Vetri. J. Colloid Interface Sci. 304(2), 413 (2006).

[12] F. Atay, V. Bilgin, I. Akyuz, S. Kose.Materials Science in Semiconductor Procesing.153 6(4), 197 (2003).

[13] R. Amutha, M. Muruganandham, G.J. Lee, and J.J. Wu. J. Nanosci. Nanotechnol.11(9), 7940 (2011).

[14] M.J. Pawar, A.D. Ingle, *Photodegradation of Acid Red 183 Dye over Ag-CdS Nanoparticles.*Chemical Science Transactions 5(3) (**2016**)645-650.

[15] M. Mall, L. Kumar J. Lumin. **130** (2010) 660.

[16] A. I. Oliva, O. Soliscanto, R. Castrorodriguez, P.Quintana Thin Solid Films **391** (2001) 28.

[17] J. I. Pankove Optical Processes in Semiconductors, Prentice Hall, Inc.,Englewood Cliffs, New Jersey, USA (1971) pp. 34.

[18] Alaton, I.A.; Balcioglu, I.A. Photochemical and Heterogeneous photocatalytic degradation of waste vinylsulphone dyes: A case study with hydrolysed Reactive Black 5. *J. Photochem. Photobiol. A Chem.* **2001**, *141*, 247-254.

[19] Daneshvar, N.; Salari, D.; Khataee, A.R. Photocatalytic degradation of azo dye acid red 14 in water: investigation of the effect of operational parameters. *J. Photochem. Photobiol. A Chem.* **2003**, *157*, 111-116.

[20] Grzechulska, J.; Morawski, A.W. Photocatalytic decomposition of azo-dye acid black 1 in waterover modified titanium dioxide. *Appl. Catal. B* **2002**, *36*, 45-51.

[21] Carter, S.R.; Stefan, M.I.; Bolton, J.R.; Safarzadeh-Amiri, A. UV/H_2O_2 Treatment of methyl tertbutylether in contaminated waters. *Environ. Sci. Technol.* **2000**, *34*, 659-662.

[22] Malato, S.; Blanco, J.; Ritchter, C.; Braun, B.; Maldonado, M.I. Enhancement of the rate of solarphotocatalytic mineralization of organic pollutants by inorganic oxidizing species. *Appl. Catal. B***1998**, *17*, 347-356.

[23] Wang, N.; Li, J.; Zhu, L.; Dong, Y.; Tang, H. Highly photocatalytic activity of metallic hydroxide/titanium dioxide nanoparticles prepared via a modified wet precipitation process.*J. Photochem. Photobiol. A Chem.* **2008**, *198*, 282-287.

[24] I.K.Konstantinou, T.A. Albanis, TiO_2-assisted photocatalytic degradation of azodyes in aqueous solution: kinetic and mechanistic investigations—A review,Appl. Catal. B: Environ. 49 (2004) 1–14.

[25] Simakov S.A. Tsur Y., J. Nanopart. Research, 9 (2007) 403.

[26] Mehrotra, K.; Yablonsky, G.S.; Ray, A.K. Macro kinetic studies for photocatalytic degradation of benzoic acid in immobilized systems. Chemosphere 2005, 60, 1427–1436.

[27] Hashimoto, K.; Irie, H.; Fujishima, A. TiO_2 Photocatalysis: A Historical Overview and Future Prospects. Jpn. J. Appl. Phys. 2005, 44, 8269–8285.

[28] Barakat, N.A.M.; Kanjwal, M.A.; Chronakis, I.S.; Kim, H.Y. Influence of temperature on the photodegradation process using Ag-doped TiO_2 nanostructures: Negative impact with the nanofibers. J. Mol. Catal. A Chem. 2013, 366, 333–340.

[29] Shams-Ghahfarokhi, Z.; Nezamzadeh-Ejhieh, A. As-synthesized ZSM-5 zeolite as a suitable support for increasing the photoactivity of semiconductors in a typical photodegradation process. *Mater. Sci. Semicond. Process*. 2015, 39, 265–275.

[30] O. Carp, C.L. Huisman,A. Reller, Photoinduced reactivity of titanium oxide photoinducedreactivity of titanium oxide, *Solid State Chem*. 32 (2004) 33–177.

[31] H.M. Coleman, V. Vimonses, G. Leslie, R. Amal, Degradation of 1,4-dioxanein water using TiO_2 based photocatalytic and H_2O_2/UV processes, *J. Hazard.Mater*. 146 (2007) 496–501.

[32] N.M. Mahmoodi, M. Arami, N.Y. Limaee, N.S. Tabrizi, Kinetics of heterogeneousphotocatalytic degradation of reactive dyes in an immobilized TiO_2photocatalytic reactor, *J. Colloid Interf. Sci*. 295 (2006) 159–164.

[33] K. Tanaka, T. Hisanaga, K. Harada, Efficient photocatalytic degradation of chloralhydrate in aqueous semiconductor suspension, *J. Photochem. Photobiol. A:Chem*. 48 (1989) 155–159.